Tantalum etching with a nonthermal atmospheric-pressure plasma

V. J. Tu, J. Y. Jeong, A. Schütze, S. E. Babayan, and G. Ding
Chemical Engineering Department, University of California, Los Angeles, California 90095

G. S. Selwyn
Plasma Physics, Los Alamos National Laboratory, Los Alamos, New Mexico 87545

R. F. Hicks[a)]
Chemical Engineering Department, University of California, Los Angeles, California 90095

(Received 28 April 2000; accepted 24 July 2000)

Tantalum was etched in a downstream, atmospheric-pressure plasma. In this process, etching occurred without significant ion bombardment. An etching rate of 6.0 ± 0.5 μm/min was achieved using 14.8 Torr oxygen, 22.4 Torr carbon tetrafluoride, 720 ± 5 Torr helium, 685 W radio frequency power at 13.56 MHz, and a film temperature of 300 °C. The etching rate increased with the applied power, carbon tetrafluoride pressure, oxygen pressure, and residence time of the gas between the electrodes, indicating that the surface reaction depends on the density of reactive fluorine species generated in the plasma. X-ray photoemission spectroscopy revealed that the etched surface was covered with tantalum fluoride and to a lesser extent, tantalum oxide. Based on these observations, a mechanism for tantalum etching is proposed which involves the reaction between fluorine atoms and the adsorbed tantalum fluoride. © *2000 American Vacuum Society.* [S0734-2101(00)01806-6]

I. INTRODUCTION

Thin films of tantalum have been used for several purposes in solid-state electronic devices. Consequently, etching processes have been developed to pattern these films into useful device structures.[1–8] Tantalum etching is also of interest for the decontamination and decommissioning of nuclear waste.[9,10] A number of researchers have investigated the dry etching of tantalum and related compounds in low-pressure plasma reactors.[1–3,10–16] These reactors, while being well suited for semiconductor processing, have some disadvantages in other applications. For example, a vacuum system can be expensive and difficult to use when the materials to be processed are large and contain surfaces that undergo continuous out-gassing. Therefore, we have decided to study this problem, and in this article, we present a report on tantalum etching with a downstream, nonthermal atmospheric-pressure plasma.

Recently, an atmospheric-pressure plasma has been developed that produces a stable, homogeneous, capacitive discharge without any filamentary arcs.[17–22] This discharge generates approximately 10^{11} charged particles per cubic centimeter at an electron temperature of $\sim$2 eV and a neutral temperature of 100–200 °C, depending on the operating conditions.[19,22] In this article, we examine the use of this source for tantalum etching. The effect of the process conditions on the reaction rate has been determined. In addition, the plasma and metal surface have been probed by optical emission spectroscopy and x-ray photoelectron spectroscopy, respectively. It is observed that the metal becomes highly fluorinated during etching, a phenomenon which is not observed in low-pressure plasma reactors.[3,12] An etching mechanism is proposed based on the experimental results.

[a)]Author to whom correspondence should be addressed; electronic mail: rhicks@ucla.edu

II. EXPERIMENTAL METHODS

The experimental apparatus has been described in a previous publication.[17] It consists of two concentric metal electrodes 15.0 cm in length. The inner electrode was 1.27 cm in diameter and was biased with a radio frequency (rf) power supply at 13.56 MHz. The outer electrode was separated from the inner electrode by a gap 0.16 cm and was grounded. This electrode was equipped with a cooling jacket through which water flowed at 20 °C. The feed gas, consisting of carbon tetrafluoride, oxygen, and helium, was passed through the annular space between the electrodes, converted into a plasma, and then directed onto a piece of polycrystalline tantalum foil located several millimeters downstream. The plasma exited through a nozzle 4.9 mm in diameter at 52 L/min, or at a linear velocity of 46 m/s (at 295 K and 1 atm).

The sample was positioned perpendicular to the flow on a stage containing two 250 W cartridge heaters attached to a temperature controller. The temperature was measured with a thermocouple attached to the back of the sample. At atmospheric pressure, the heat from the highly exothermic etching reaction does not appreciably change the sample temperature, because at steady state, this heat is transferred to the metal holder and the flowing helium gas. The amount of heat transfer to the gas can be estimated by Newton's law of cooling: $q=hA\Delta T$, where A is the etching area, ΔT is the temperature change, and h is the heat transfer coefficient ($\sim$50 kcal/m^2 h °C).[23] Assuming an overall reaction of $5F+Ta\rightarrow TaF_5+510$ kcal/mol, an etching rate of 1 μm/min, and no heat transfer to the sample holder, a thermal energy balance yields a maximum temperature rise of 37 K. In this calculation, conduction between the sample and holder has been neglected, because the contact between the two is not known with certainty. Nevertheless, neglecting this contribution to the heat loss yields a conservative estimate of the temperature rise. Thus, the temperature of the tantalum sur-

face was slightly higher than the value measured by the thermocouple (i.e., 500–650 K), but well within 37 K, or a maximum error of 7.4%.

Etching was restricted to a circular area 65.7 mm^2 by an aluminum mask. The tantalum foil was 99.95% pure with a thickness of 12.7 μm and a density of 16.6 g/cm^3 (Alpha Aesar, Stock No. 14266). The etching rate was determined by measuring the time it took to punch through the foil, which varied from 2 to 25 min. The etching rate was fairly uniform since the entire area was removed within 10 s after the hole first appeared. Consequently, the experimental error in this technique was less than 10%.

The reactive species generated between the electrodes was identified by optical emission spectroscopy. Spectra were collected with a monochrometer equipped with a charge coupled device camera, at a resolution of 1 Å, and using an entrance slit 0.15 mm in width. A mirror, mounted 5 mm downstream of the electrodes, collected all the light emanating from the plasma and directed it through a lens and into the entrance slit.

The tantalum surface composition before and after etching was analyzed with a PHI 5000 x-ray photoemission spectrometer (XPS), equipped with a hemispherical analyzer and a multichannel detector. Spectra were recorded at a take-off angle of 55° with respect to the sample normal using Al K_α x rays and a pass energy of 23.5 eV. Surface measurements were made *in situ*, in which the sample was transferred directly to the XPS without air exposure, and *ex situ*, in which the sample was exposed to the laboratory air during transfer from the plasma reactor to the XPS. The *in situ* measurements were made with the plasma jet installed in an ultrahigh vacuum chamber that was connected to the analytical chamber via a planetary sample-transfer system.[24] After mounting the sample in the vacuum chamber, it was backfilled with argon from 5×10^{-7} to 760 Torr, and the sample was etched for 5 min with a carbon tetrafluoride, oxygen, and helium plasma. Then, the chamber was pumped out and the sample transferred to the XPS for analysis. *Ex situ* etching was carried out in a small reactor that was backfilled with helium from 0.02 to 760 Torr before turning on the plasma. The etching reaction was carried out for 5 min under the same operating conditions as in the *in situ* case. Then the tantalum sample was removed and carried across the room to a loadlock, where it was mounted on a holder and transferred to the XPS system.

III. RESULTS

A. Effect of process conditions on etching rate

The effect of the rf power on the tantalum etching rate is shown in Fig. 1. The process conditions were 15.5 Torr CF_4, 14.2 Torr O_2, 725±5 Torr He, 250 °C sample temperature, and a nozzle-to-sample distance of 3 mm. With these relatively high concentrations of carbon tetrafluoride and oxygen, the plasma flickers and begins to extinguish when the rf power is dropped below 300 W. On the other hand, the rf power cannot be increased above 650 W, otherwise arcing occurs and damages the electrodes. Within the allowable operating window, the etching rate increases rapidly with the applied power. A log–log plot of the data yields the following dependence of the rate on power: $R_{\mathrm{etch}} \propto P_{\mathrm{rf}}^{2.4}$. These data show that the production rate of reactive species within the plasma strongly influences the etch rate of tantalum placed downstream of the source.

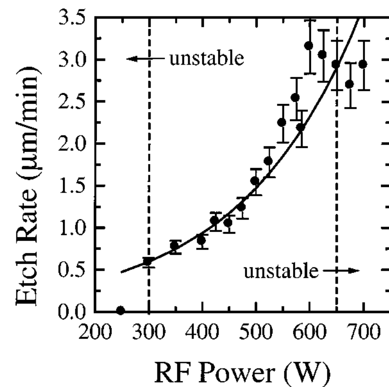

FIG. 1. Dependence of the etching rate on applied power. (The conditions were 15.5 Torr CF_4, 14.2 Torr O_2, 725±5 Torr He, 250 °C sample temperature, and a nozzle-to-sample distance of 3 mm.)

The dependence of the tantalum etching rate on the partial pressure of carbon tetrafluoride is shown in Fig. 2. The process conditions were 500 W rf power, 11.4 Torr O_2, 735±10 Torr He, 300 °C sample temperature, and a nozzle-to-sample distance of 3 mm. The reaction rate increases linearly with the CF_4 pressure up to 20 Torr. Beyond this value, arcing occurs and the plasma can no longer be operated. Presented in Fig. 3 is the dependence of the etching rate on the oxygen partial pressure. The process conditions in this case were 300 W rf power, 15.5 Torr CF_4, 735±10 Torr He, 300 °C sample temperature, and a nozzle-to-sample distance of 5 mm. A sudden rise in the etching rate is recorded as the oxygen pressure is raised from 0 to 5 Torr. Then the rate levels off at 2.0 μm/min as the O_2 pressure is increased from 5 to 20 Torr. Injection of oxygen into a CF_4 plasma is known to accelerate the production of fluorine atoms.[25,26,30] Therefore, the behavior exhibited in Figs. 2 and 3 indicates a direct

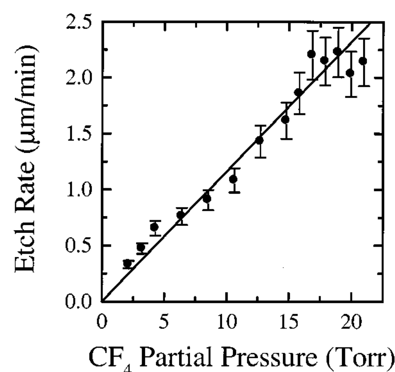

FIG. 2. Dependence of the etching rate on CF_4 partial pressure. (The conditions were 500 W rf power, 11.4 Torr O_2, 735±10 Torr He, 300 °C sample temperature, and a nozzle-to-sample distance of 3 mm.)

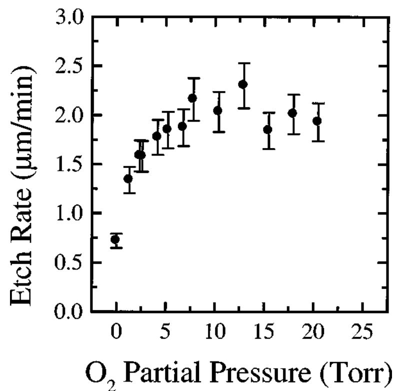

FIG. 3. Dependence of the etching rate on the oxygen partial pressure. (The conditions were 300 W rf Power, 15.5 Torr CF_4, 735±10 Torr He, 300 °C sample temperature, and a nozzle-to-sample distance of 5 mm.)

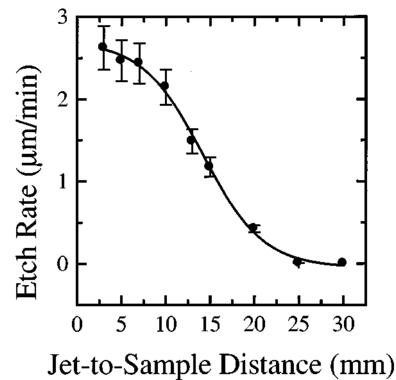

FIG. 5. Dependence of the etching rate on the nozzle-to-sample distance. (The conditions were 500 W rf power, 15.5 Torr CF_4, 11.4 Torr O_2, 730±5 Torr He, and 300 °C sample temperature.)

correlation between the production rate of fluorine atoms in the plasma and the etching rate of tantalum placed in the downstream ''afterglow'' region.

The dependence of etching rate on the gas residence time between the electrodes is presented in Fig. 4. Here, the conditions were 300 W rf power, 15.5 Torr CF4, 11.4 Torr oxygen, 735±5 Torr He, 300 °C sample temperature, and a nozzle-to-sample distance of 5 mm. A linear dependence between rate and residence time is observed. These results further show that the etching rate depends directly upon the amount of reactive fluorine species, e.g., F atoms, generated in the plasma, and not simply on the feed rates of CF_4 and O_2 to the system.

The effect of the nozzle-to-sample distance on the tantalum etching rate is shown in Fig. 5. The plasma was operated at 500 W rf power, 15.5 Torr CF_4, 11.4 Torr O_2, 730±5 Torr He, and 300 °C sample temperature. The etching rate decays nonlinearly with distance from the source. Out to about 5 mm, the rate decreases only a small amount, whereas from 5 to 25 mm it rapidly drops to 0. It should be noted that ions play a negligible role in the etching reaction, as confirmed in sample biasing experiments, in which no change in the etch rate occurred with varying the bias on the Ta foil from +200 to −200 V. This phenomenon can be explained by the low charge flux (10^{14} cm^2/s) in the downstream region.[18] The maximum etching rate that can be induced by this flux is less than 0.1 μm/min, assuming one electron charge removes one tantalum atom. Since the etching rates range from 0.5 to 6.0 μm/min, ions cannot be contributing significantly to the process.

The effect of the sample temperature upon the etching rate is shown in Fig. 6. The process conditions were 300 W rf power, 15.5 Torr CF_4, 11.4 Torr O_2, 735±10 Torr He, and a nozzle-to-sample distance of 5 mm. The temperature of the plasma effluent gas is 225 °C, which establishes the lower bound for this experiment. Upon raising the temperature from 225 to 375 °C, the etching rate increases slightly from 0.9 to 1.5 μm/min. The apparent activation energy calculated from the slope of the line is 2.3±0.7 kcal/mole. Activation energies reported in the literature for reactive ion etching of tantalum at low pressure range from 0.7 to 5.6 kcal/mol.[3,10]

B. Optical emission spectra of the plasma

Since this is the first report of tantalum etching with a nonthermal, atmospheric-pressure plasma, optical emission spectra were collected to obtain a fingerprint of the chemical

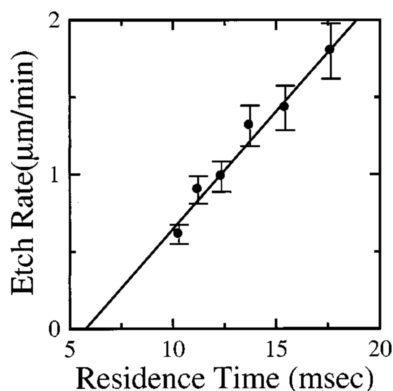

FIG. 4. Dependence of the etching rate on the residence time of the gas in the plasma. (The conditions were 300 W rf power, 15.5 Torr CF_4, 11.4 Torr oxygen, 735±5 Torr He, 300 °C sample temperature, and a nozzle-to-sample distance of 5 mm.)

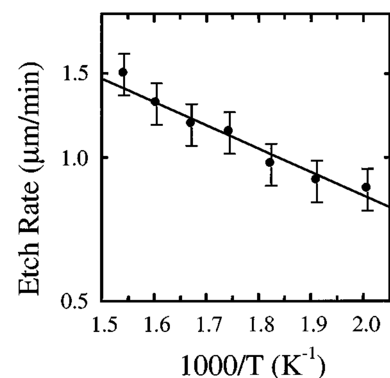

FIG. 6. Dependence of the etching rate on temperature between 225 and 375 °C. (The conditions were 300 W rf power, 15.5 Torr CF_4, 11.4 Torr O_2, 735±10 Torr He, and a nozzle-to-sample distance of 5 mm.)

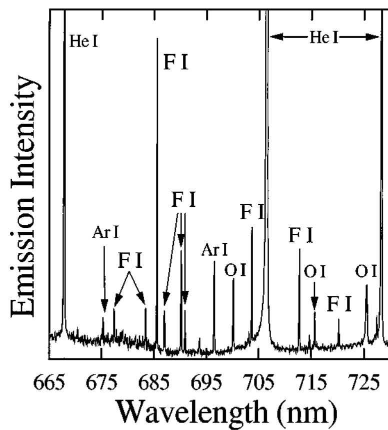

FIG. 7. Optical emission spectrum of the atmospheric-pressure plasma operated with a carbon tetrafluoride, oxygen, and helium gas mixture. (The conditions were 150 W rf power, 0.2 Torr CF_4, 3.1 Torr O_2, and 755±5 Torr He.)

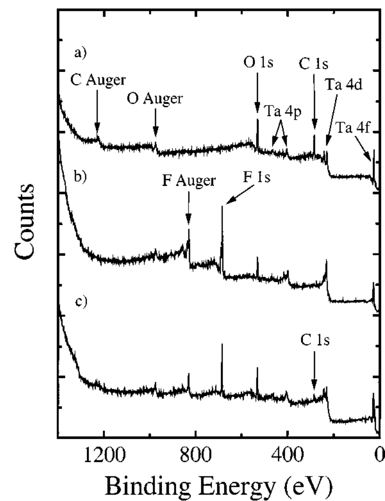

FIG. 8. Survey photoemission spectra of the tantalum surface (a) before etching, (b) after etching with *in situ* analysis, and (c) after etching with *ex situ* analysis.

species in the discharge. A spectrum recorded between 665 and 750 nm is shown in Fig. 7. The emission is very weak, requiring integration over 3.0 s to obtain a reasonable signal-to-noise ratio. The weak signal is most likely due to rapid collisional quenching of the excited species at atmospheric pressure. In this experiment, the conditions were 150 W rf power, 0.2 Torr CF_4, 3.1 Torr O_2, and 755±5 Torr He. Intense bands are observed for electronically excited helium atoms $3d^1D$, $3s^3S$ and $3s^1S$ (at 667.82, 706.52, 706.57, and 728.14 nm), fluorine atoms $3p^4D$ and $3p^2P$ (at 677.4, 683.4, 687.02, 690.25, 690.98, 703.7, 712.79, and 720.24 nm), oxygen atoms $4d^3D$ $3p^1D$ and $5s^3S$ (at 700.192, 700.223, 715.67, 725.42, 725.44, and 725.45 nm) and argon atoms $3S^23p^5(^2P^0_{3/2})5d$ and $3S^23p^5(^2P^0_{1/2})4d$ (at 675.28 and 696.54 nm).[25] In addition, emission from metastable oxygen molecules ($b\,^1\Sigma_g^+ O_2 \rightarrow X\,^3\Sigma_g^- O_2$) is recorded at 758–770 nm. The fluorine and oxygen atom emission observed in this study is qualitatively similar to that seen in a parallel-plate discharge operating at 0.4 Torr with 92 vol % CF_4 and 8 vol % O_2.[26,27] These results confirm that fluorine and oxygen atoms are produced from the carbon tetrafluoride and oxygen molecules fed to the plasma. However, since the emission is due to electronically excited species, it is not straightforward to calculate the ground-state concentrations of the atoms, especially for this highly collisional plasma.

C. X-ray photoemission spectra of the tantalum surface

Survey spectra taken of the tantalum surface before and after plasma etching are shown in Fig. 8. Here, the discharge was operated at 500 W rf power, 15.5 Torr CF_4, 10.4 Torr O_2, 730±5 Torr He, 250 °C sample temperature, and a nozzle-to-sample distance of 5 mm. Before exposure, one sees peaks at 1226 and 285 eV due to carbon Auger and 1*s* photoemission, at 978 and 532 eV due to oxygen Auger and 1*s* photoemission, and at 570±5, 465±3, 405±3, 240±2, 230±2, and 25±4 eV due to tantalum *4s*, $4p_{1/2}$, $4p_{3/2}$, $4d_{5/2}$, and $4f$ photoemission.[28] After etching, the spectrum recorded *in situ* [Fig. 8(b)] contains two additional peaks at 830 and 685 eV due to the fluorine Auger and 1*s* lines. In addition, the O 1*s* peak is much smaller than that recorded before etching and the C 1*s* peak is below the detection limit. The spectrum obtained *ex situ* after etching is similar to that obtained *in situ*, except that the C 1*s* peak is now clearly visible at 285 eV.

Listed in Table I is the composition of the tantalum surface measured by XPS before and after etching. The composition was calculated using the atomic sensitivity factors provided by Physical Electronics for our hemispherical analyzer. Before etching, the tantalum is covered mainly with carbon (43.1 at. %) and oxygen (37.2 at. %). After etching, *in situ* analysis reveals that the metal is highly fluorinated with a coverage corresponding to 73.9 at. % fluorine. In addition, the adsorbed carbon is below 2.0 at. %, which is the detection limit of the spectrometer. These data show that a fluorocarbon polymer film is not deposited on the sample, as is sometimes seen in low-pressure plasma etchers.[3] Exposure to air immediately after etching causes the fluorine coverage to decrease by half and the carbon coverage to increase by nearly fourfold. Evidently, the fluorinated layer is susceptible to attack by molecules found in the ambient environment, such as water, hydrocarbons, and carbon dioxide.

Shown in Fig. 9 are high-resolution photoemission spectra of the tantalum $4f_{5/2}$ and $4f_{7/2}$ states. These spectra contain a series of overlapping bands due to the presence of different

TABLE I. Average composition of the tantalum surface (at. %).

Element	Before etching	After etching *(in situ)*	After etching *(ex situ)*
Tantalum	19.8	5.3	26.0
Oxygen	37.2	18.8	21.3
Fluorine	0.0	73.9	37.7
Carbon	43.1	<2.0	15.1

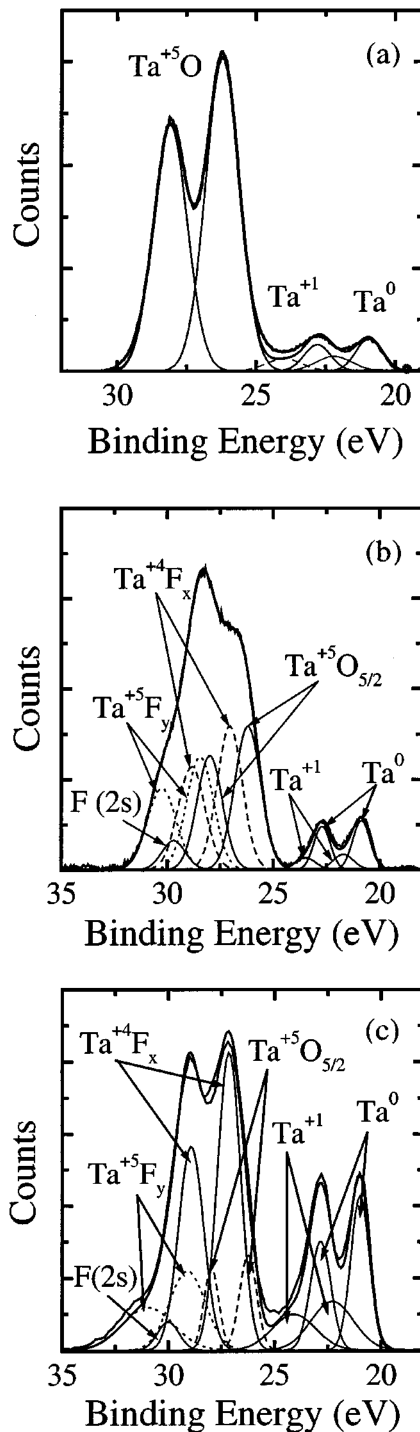

FIG. 9. Tantalum $4f_{7/2}$ and $4f_{5/2}$ photoemission spectra of the metal surface (a) before etching, (b) after etching with *in situ* analysis, and (c) after etching with *ex situ* analysis.

tantalum oxidation states. The binding energy scale has been fixed by referencing the $4f_{7/2}$ peak for metallic tantalum, Ta^0, to 20.9 eV.[3,28] Deconvolution of these bands was performed with the Multipak data analysis suite.[29] Each individual chemical state yields a doublet split corresponding to the $4f_{7/2}$ and $4f_{5/2}$ lines. These lines are separated by 1.8 eV and exhibit a fixed area ratio of $A_{Ta_{7/2}}/A_{Ta_{5/2}}=4/3$. The peak shapes were determined using a Gaussian–Lorentzian model

TABLE II. Percentage of tantalum that is contained within each chemical state $[100(Ta_i/\Sigma Ta_i)]$.

State		After etching	
($4f_{7/2}$, $4f_{5/2}$ eV)	Before etching	(*in situ*)	(*ex situ*)
Ta^0 (20.9, 22.7)	5.2	7.5	19.4
Ta^{+1} (21.7, 23.5)	8.1	2.6	14.7
$Ta^{+5}O$ (26.2, 28.0)	86.7	32.3	15.0
$Ta^{+4}F_x$ (27.0, 28.8)	0.0	31.2	36.0
$Ta^{+5}F_y$ (28.5, 30.3)	0.0	26.3	14.9
Total:	100.0	100.0	100.0

supplied with the Multipak software. It should be noted that the O 2*s* peak at 23.0 eV does not contribute significantly to these spectra because its sensitivity factor is very low (0.035).

Before etching [Fig. 9(a)], three doublets are observed due to Ta^0, Ta^{+1} suboxide or carbide, and Ta^{+5} oxide.[3,12,28,30,31] The Ta $4f_{7/2}$ binding energies for these three states are 20.9, 21.7 and 26.2 eV, respectively. The Ta^{+1} designation is provided to distinguish this feature from Ta^0, and is not meant to indicate the formal valence on the atom. This band most likely arises from oxygen or carbon adsorbed on tantalum, as distinguished from the bulk metal.[30] Shown in Table II is the distribution of the tantalum among these different states. These percentages have been calculated by taking the ratio of the area under a particular $4f_{7/2}$ band to that under all the $4f_{7/2}$ bands. Before etching, about 85% of the metal atoms sampled by the spectrometer are present as Ta_2O_5. These results are consistent with previously published data on tantalum foils exposed to air.[3,12,15]

After etching, *in situ* XPS [Fig. 9(b)] reveals that there are two new Ta $4f_{7/2}$ peaks at 27.0 and 28.5 eV. These new features are due to fluorinated tantalum, and are assigned to metal fluorides or oxyfluorides in the +4 and +5 valence states.[13,28] The distribution of tantalum among the different chemical species is shown in Table II, third column. Tantalum fluorides and oxyfluorides comprise 57.5% of the surface sampled, whereas tantalum oxide comprises 32.3%. The remainder is divided between Ta^0 and Ta^{+1}. The TaF_x states appearing at binding energies above that of Ta_2O_5 have not been observed in previous studies of plasma etching of tantalum metal.[3,12] Since there is a significant concentration of tantalum fluorides on the surface, it is likely that the etching process is limited by the surface reaction of fluorine species, e.g., F atoms, with this metal fluoride layer.

In Fig. 9(c), the Ta 4*f* spectrum is presented for a sample exposed to room air after the etching reaction. The same chemical states are present on this surface as on the one analyzed *in situ*, except that the relative intensities of the peaks have changed. Referring to Table II, column 4, the tantalum compounds in 5+ oxidation states (Ta_2O_5 and

$Ta^{+5}F_y$) have decreased, while the tantalum metal and Ta compounds in lower oxidation states (Ta^0, Ta^{+1}, and $Ta^{+4}F_x$) have increased. The changes to the Ta 4*f* spectrum caused by air exposure were reproduced for at least six measurements, and were found to be insensitive to the duration of the exposure, which was varied from 5 min to 2 h. These data indicate that the chemical composition of the fluoride layer on the tantalum surface is sensitive to the gas environment and exists in a higher average oxidation state under the flux of fluorine species generated from the atmospheric pressure plasma.

IV. DISCUSSION

To summarize the results presented earlier, we observe that the rate of tantalum etching at atmospheric pressure strongly depends on the operation conditions of the gas discharge. In particular, the Ta stripping rate increases with rf power, CF_4 concentration, O_2 concentration, gas residence time between the electrodes, and sample temperature. The observed trends suggest that fluorine atoms are the active species responsible for etching the tantalum surface. For example, it is well known that oxygen accelerates the production of fluorine atoms from carbon tetrafluoride by oxidizing CF_x radicals into carbon oxides and F atoms.[25,26,30] On the other hand, the rate was unaffected by the sample bias from +200 to −200 V. This is expected for a high-pressure downstream source, where essentially all the ions are consumed by reactions prior to reaching the substrate.

A number of studies have been published on tantalum etching in low-pressure gas discharges (<0.5 Torr).[1,3,10–12,15] In this case, the rate of tantalum etching depends on the gas composition, applied rf power, bias power, temperature, and total pressure. For CF_4 and O_2 plasmas, there is a complex dependence of the etching rate on the oxygen pressure. Initially, the rate increases with the amount of O_2 added, presumably because the O atoms oxidize away a fluorocarbon layer that inhibits the etching process.[15] Then, with further increases in the amount of oxygen fed to the plasma, the etch rate reaches a maximum and declines. Hsiao and Miller[15] have proposed that at the higher oxygen concentrations, the tantalum is converted into a tantalum oxide that exhibits a reduced etching rate. This chemistry does not appear to occur in the atmospheric-pressure plasma examined herein. The XPS data reveal that no appreciable amount of carbon is deposited on the surface during etching. In addition, the surface is always covered with tantalum fluoride, regardless of the amount of oxygen fed to the plasma discharge.

In the atmospheric-pressure plasma process, the rate of tantalum etching appears to depend on the flux of fluorine atoms to the sample surface. However, the XPS data show that the metal surface is heavily fluorinated during this reaction. Because of this, it is unlikely that either transport or adsorption of fluorine species is rate limiting. Otherwise, the reactions following these steps would occur rapidly on the surface and drive the adsorbed fluorine concentration to 0. Moreover, the etching rate cannot be controlled by TaF_5 sublimation, since the boiling point of this compound is 230 °C, while the substrate temperature ranges from 225 to 375 °C. If the reaction were limited by TaF_5 sublimation, the etching rate would not be sensitive to rf power, CF_4 pressure, and gas residence time, as observed. These results imply that the metal etching rate depends upon both the flux of F atoms to the surface and the existence of the TaF_x surface layer.

Two alternative reaction mechanisms may be proposed which are consistent with our results. (a) The reaction may follow an Eley–Rideal mechanism in which gas-phase fluorine atoms collide directly with the adsorbed metal fluoride in the rate-limiting step

$$F_{(g)} + TaF_{x(s)} \rightarrow TaF_{x+1(s)}. \quad (1)$$

The subscripts *g* and *s* refer to gaseous and adsorbed species. The production of TaF_5 may occur in this step, or in a later step with a faster intrinsic rate. (b) Fluorine atoms may weakly chemisorb onto the surface, and then slowly react with tantalum fluoride to make the reaction products

$$F_{(g)} \leftrightarrow F_{(s)}, \quad (2)$$

$$F_s + TaF_{x(s)} \rightarrow TaF_{x+1(g)}. \quad (3)$$

In reaction (2), fluorine atoms adsorb on top of the metal fluoride layer. Then they diffuse across the surface until they collide with a TaF_x species in the rate-limiting step, reaction (3). The latter mechanism is consistent with the results of Machiels and Olander,[32] who examined the reaction of fluorine molecules with tantalum foil by modulated molecular beam-mass spectrometry. An analysis of their data indicated that the fluorine dissociatively adsorbs onto a scale composed of a tantalum subfluoride. Then the F atoms diffuse through the scale and react with specific sites to produce TaF_5. In the case of tantalum etching with the downstream, atmospheric-pressure plasma, further work is needed to determine which of the proposed reaction mechanisms dominates.

V. CONCLUSIONS

We have investigated the etching of polycrystalline tantalum foil with a nonequilibrium, atmospheric-pressure plasma. Rates up to 6.0 μm/min have been obtained in the absence of ion bombardment. The effects of the operation conditions on stripping rates have been determined. An analysis of the experimental results suggests that the etching rate is limited by the reaction of fluorine atoms with tantalum subfluoride on the surface of the metal substrate.

ACKNOWLEDGMENTS

This work was conducted under the auspices of the US Department of Energy, supported in part by funds provided by the University of California, and in part by funds provided by Basic Energy Sciences, Environmental Management Sciences Program, and the Office of Science and Risk Policy (Award No. DE-F5607-96ER45621). J.J. and S.B. are grateful for fellowships from the University of California Center for Environmental Risk Reduction and the Toxic

Substances Research and Training Program. A.S. is grateful for a Fellowship from the Deutsche Forschungsgemeinschaft (DFG).

[1] A. Picard and G. Turban, Plasma Chem. Plasma Process. **5**, 333 (1985).
[2] T. P. Chow and A. J. Steckl, *4th Symposium on Plasma Processing, San Francisco, CA* (Electrochemical Society, Pennington, NJ, 1983), p. 362.
[3] Y. Kuo, Jpn. J. Appl. Phys., Part 1 **32**, 179 (1993).
[4] B. W. Shen, I. Chen, S. Banerjee, G. A. Brown, J. Bohlman, P.-H. Chang, and R. R. Doering, 1987 International Devices Meeting, Washington, DC, 1987, p. 582.
[5] Y. Kuo, SPIE Display SystemOptics II **1117**, 114 (1989).
[6] P. Singer, Semicond. Int. **22**, 34 (1999).
[7] P. Singer, Semicond. Int. **21**, 90 (1998).
[8] C. Chaneliere, J. L. Autran, R. A. B. Devine, and B. Balland, Mater. Sci. Eng., R. **R22**, 269 (1998).
[9] J. C. Martz, D. W. Hess, J. M. Haschke, J. W. Ward, and B. F. Flamm, J. Nucl. Mater. **182**, 277 (1991).
[10] J. C. Martz, D. W. Hess, and W. E. Anderson, J. Appl. Phys. **67**, 3609 (1990).
[11] D. E. Ibbotson, J. A. Mucha, D. L. Flamm, and J. M. Cook, Appl. Phys. Lett. **46**, 794 (1985).
[12] Y. Kuo, J. Electrochem. Soc. **139**, 579 (1992).
[13] J. H. Thomas, III and L. H. Hammer, J. Electrochem. Soc. **136**, 2004 (1989).
[14] S. P. Sun and S. P. Murarka, J. Electrochem. Soc. **135**, 2353 (1988).
[15] R. Hsiao and D. Miller, J. Electrochem. Soc. **143**, 3266 (1996).
[16] R. Hsiao, D. Miller, T. Lin, and N. Robertson, Thin Solid Films **304**, 381 (1997).
[17] J. Y. Jeong, S. E. Babayan, V. J. Tu, J. Park, I. Henins, J. Velarde, R. F. Hicks, and G. S. Selwyn, Plasma Sources Sci. Technol. **7**, 282 (1998).
[18] S. E. Babayan, J. Y. Jeong, V. J. Tu, J. Park, R. F. Hicks, and G. S. Selwyn, Plasma Sources Sci. Technol. **7**, 286 (1998).
[19] A. Schütze, J. Y. Jeong, S. E. Babayan, J. Park, G. S. Selwyn, and R. F. Hicks, IEEE Trans. Plasma Sci. **26**, 1685 (1998).
[20] J. Y Jeong, S. E. Babayan, A. Schütze, V. J. Tu, J. Y. Park, I. Henins, G. S. Selwyn, and R. F. Hicks, J. Vac. Sci. Technol. A **17**, 2581 (1999).
[21] H. W. Hermann, I. Henins, J. Park, and G. S. Selwyn, Phys. Plasmas **6**, 2284 (1999).
[22] J. Park, J. Y. Jeong, C. S. Chang, I. Henins, H. W. Herrmann, D. S. Shim, R. F. Hicks, and G. S. Selwyn, Appl. Phys. Lett. **76**, 288 (2000).
[23] R. B. Bird, W. E. Stewart, and E. N. Lightfoot, *Transport Phenomena* (Wiley, New York, 1966).
[24] L. Li, B. K. Han, S. Gan, H. Qi, and R. F. Hicks, Surf. Sci. **398**, 386 (1998).
[25] J. Reader and C. H. Corliss, Nat. Stand. Ref. Data Ser., Nat. Bur. Stand., 1980.
[26] W. R. Harshbarger, R. A. Porter, T. A. Miller, and P. Norton, Appl. Spectrosc. **31**, 201 (1977).
[27] W. R. Harshbarger and R. A. Porter, Solid State Technol. **21**, 99 (1978).
[28] *Handbook of X-ray Photoelectron Spectroscopy*, edited by C. D. Wagner, W. M. Riggs, L. E. Davis, J. F. Moulder, and G. E. Muilenberg (Perkin-Elmer, Eden Prairie, MN, 1979).
[29] Multipak Version 2.2 (Physical Electronics, Inc., Eden Prairie, MN, 1996).
[30] J. F. van der Veen, F. J. Himpsel, and D. E. Eastman, Phys. Rev. B **25**, 7388 (1982).
[31] J. W. Coburn and H. F. Winters, J. Vac. Sci. Technol. **16**, 391 (1979); T. D. Bestwick and G. S. Oehrlein, J. Appl. Phys. **66**, 5034 (1989).
[32] A. J. Machiels and D. R. Olander, Surf. Sci. **65**, 325 (1977).